Polarization Sensing with Transmission Fibers in Undersea Cables

Antonio Mecozzi,[1,*] **Mattia Cantono,**[2] **Jorge C. Castellanos,**[2,3] **Valey Kamalov,**[3] **and Zhongwen Zhan**[3]

[1]*Department of Physical and Chemical Sciences, University of L'Aquila, L'Aquila 67100, Italy*
[2]*Google Inc., USA*
[3]*Seismological Laboratory, California Institute of Technology, Pasadena, USA*
[*]*antonio.mecozzi@univaq.it*

Abstract: We show that from the state of polarization of the received signal transmitted in an undersea cable, information on geophysical events occurring on the ocean floor and surface can be extracted without disturbing the ongoing data communication. © 2021 The Author(s)

1. Introduction

Optical communication systems have evolved from legacy on-off keying to present days coherent systems. Such systems require, for their operation, the characterization of the optical channel, namely of the propagation through the optical fiber. This propagation is affected by perturbations from the environment, and the real-time channel characterization can be used as a sensing tool for those perturbations [1]. Key to this task is the characterization of the effect of those perturbations on the propagation of the light along the fiber [2].

2. Phase and SOP sensitivity to strain of SSMF

The use of optical fibers for geophysical sensing is not new. Indeed, one of the most successful fiber-optic based technique for geophysical sensing is distributed acoustic sensing (DAS) [3]. This technique is based on the time-resolved measurement of the phase of the Rayleigh backscattered signal, which is modulated by the time-dependent interaction of the fiber with the environment. The phase accumulated by the Rayleigh backscattered light over a roundtrip is twice the phase accumulated one way. Recently, a number of measurement campaigns based on the use of DAS in standard (armored or lightwave) submarine cables experimentally characterized the dependence of the phase accumulated during the roud-trip on external perturbations [4–6]. Useful information on the dependence of the state of polarization (SOP) on the perturbation can therefore be gained by establishing a relation between the average phase accumulated during fiber propagation and the SOP modulations at the output, because this would give us the ability to compare with DAS measurements. As we show below, this can indeed be done and the results shade light on the dependence of the SOP on external perturbations.

The propagation of the electric field of a birefringent fiber, described by the column vector $\vec{E}$, over a length ℓ much shorter than L_F, the coherence length of the birefringence, is described by [7] $\mathrm{d}\vec{E}/\mathrm{d}z = i\mathbf{H}\vec{E} = i\left(\beta_0\mathbf{I}+\vec{\beta}\cdot\vec{\sigma}/2\right)\vec{E}$, where $\vec{\sigma}$ is the Pauli matrix, with components the three Pauli matrices, $\vec{\beta}$ is the three-dimensional birefringence vector, and $\mathbf{I}$ is the two-by-two identity matrix. In the basis of the local linear eigenpolarizations, $\mathbf{H}$ is a two-by-two diagonal matrix with diagonal entries the wavevectors of the two eigenpolarizations $\beta_{1,2} = 2\pi n_{1,2}/\lambda$, where $n_{1,2}$ is the corresponding effective refractive indices. Consequently, the only non-zero component of the three dimensional vector $\vec{\beta}$ is the first, and hence $\mathbf{H} = \beta_0\mathbf{I} + (\beta/2)\,\sigma_1$, with σ_1 the diagonal Pauli matrix with 1 and -1 on the main diagonal. In this basis, $\beta_0 = (\beta_1+\beta_2)/2$ is the polarization averaged wavevector and $\beta = \beta_1 - \beta_2$ is the modulus of the birefringence vector $\vec{\beta} = (\beta,0,0)$, which is parallel to the first axis of the Stokes space because we have used the basis of the fiber eigenpolarizations [7]. We have $\beta_0 = 2\pi n/\lambda$ and $\beta = 2\pi\,\delta n/\lambda$, where $n = (n_1+n_2)/2$ is the polarization averaged effective refractive and $\delta n = n_1 - n_2$ is the difference of the effective refractive indices between the two eigenpolarizations.

Various external sources may affect the polarization averaged wavevector and the birefringence vector. Some of those apply strain to the fiber. Assume that axial strain is applied to a birefringent fiber. The key observation is that axial symmetric strain cannot rotate the birefringence axes. Strain can only change the eigenvectors β_1 and β_2 of the quantities $\Delta\beta_1 = 2\pi\Delta n_1/\lambda$ and $\Delta\beta_2 = 2\pi\Delta n_1/\lambda$, where $\Delta n_{1,2}$ are caused by the strain optic effect and by a change in the mode profile. Strain also affects the propagating distance. Both effects contribute to a change of the polarization averaged phase and of the differential phase. Let us analyze the effect on the average phase first.

The phase accumulated by light propagating over a length ℓ is $\varphi_0 = \beta_0 \ell$. Strain affects φ_0 through a change of ℓ and of β_0 and hence it produces the phase shift $\Delta\varphi_0 = \Delta\beta_0 \ell + \beta_0 \Delta\ell$, where $\Delta\beta_0 = (\Delta\beta_1 + \Delta\beta_2)/2$. This phase shift can be written as $\Delta\varphi_0 = \varepsilon_0 \varphi_0$, where $\varepsilon_0 = \Delta\beta_0/\beta_0 + \Delta\ell/\ell = \Delta(\beta_0\ell)/(\beta_0\ell)$. If $n\ell$ is the polarization averaged optical path length, than $\varepsilon_0 = \Delta(n\ell)/(n\ell)$ so that ε_0 is also the relative variation of the polarization-averaged optical path length. The quantity ε_0 can therefore be considered as an *optical* strain, as opposed to the material strain $\tilde{\varepsilon}_0 = \Delta\ell/\ell$, which is the relative variation of the fiber's geometrical length. The optical and the material strains are proportional, and their relation is characterized in the DAS literature [6] by $\varepsilon_0 = \xi\tilde{\varepsilon}_0$, where the ξ is the photoelastic scaling factor.

The three dimensional Stokes vector $\Delta\vec{\beta} = (\Delta\beta, 0, 0)$, where $\Delta\beta = \Delta\beta_1 - \Delta\beta_2 = 2\pi\Delta(\delta n)/\lambda$, quantifies the effect of strain on the birefringence vector $\vec{\beta}$. The differential phase between the two eigenpolarizations is $\varphi = \beta\ell$ and its change is $\Delta\varphi = \Delta\beta\ell + \beta\Delta\ell = \varepsilon\varphi$ where $\varepsilon = \Delta\beta/\beta + \Delta\ell/\ell = \Delta(\beta\ell)/(\beta\ell)$. Also in this case, we have that $\varepsilon = \Delta(\delta n\ell)/(\delta n\ell)$ is the relative variation of the difference between the optical path lengths of the two eigenpolarizations. Standard single mode fibers (SSMFs) are circularly symmetric and birefringence is generated by small deviations from circular symmetry caused by static perturbations frozen after drawing process. Being strain also circularly symmetric, it cannot rotate the birefringence and it mainly affects the birefringence by a change of the effective refractive indices of the two eigenpolarizations and of the fiber length. For the same symmetry reasons, it is reasonable to assume that the relative change of the fast and slow axes wavevector are on average equal, that is $\Delta\beta_1/\beta_1 = \Delta\beta_2/\beta_2 = \varepsilon_a$. Using this assumption, it is straightforward to show that $\Delta\beta/\beta = \Delta\beta_0/\beta_0 = \varepsilon_a$, and hence that $\varepsilon = \varepsilon_0 = \varepsilon_a$. The equality $\varepsilon = \varepsilon_0$ allows the characterization of the effect of strain on the polarization averaged phase from effect of strain on birefringence. This equality is not in general valid when circular symmetry is intentionally broken, like in highly birefringent fibers [8].

In the following analysis, it is convenient to keep the propagation length constant adding to $\Delta\beta$ a contribution that accounts for the change of ℓ, defining $\Delta\beta' = \Delta\beta + (\Delta\ell/\ell)\beta$. Being $\Delta\vec{\beta}'$ parallel to $\vec{\beta}$, we also have $\Delta\vec{\beta}' = \Delta\vec{\beta} + (\Delta\ell/\ell)\vec{\beta}$. Using this definition, we have $\Delta\vec{\beta}' = \varepsilon\vec{\beta}$. In the following we will always deal with $\Delta\vec{\beta}'$ and not use $\Delta\vec{\beta}$ any longer, so that we will remove the prime in $\Delta\vec{\beta}'$ for simplicity of notation.

Strain can be applied to the fiber either directly, or be the effect of external hydrostatic pressure P of the medium surrounding the fiber via the dependence of ε on P via $\varepsilon = \varepsilon_P P$, where $\varepsilon_P = \partial\varepsilon/\partial P$. It is highly unlikely that any external perturbations may directly apply strain on the fibers used in submarine system, because they are loosely housed into a jelly-filled cable. On the other hand, a recent experiment has shown a strong sensitivity to pressure variations of an optical fiber embedded in a jelly-filled cable placed on the seafloor at a depth of about 1000 m [6]. In this experiment, by comparing DAS data with a pressure sensor placed nearby, a value of $|\varepsilon_P| \simeq 36 \cdot 10^{-10}\text{Pa}^{-1}$ can be deduced. Although this value of pressure is more than one order of magnitude higher ($\varepsilon_P = -0.84 \cdot 10^{-10}\text{Pa}^{-1}$) than that theoretically predicted [9], see also [10] for a recent review, we believe that the interaction of the fiber with the cable structure, which may be resonant at acoustic frequencies, may play a role in the enhanced sensitivity.

If we neglect polarization dependent loss, the electric field at the output of a link is equal to the input electric field transformed by the action of a two-by-two unitary matrix $\mathbf{U}(z)$, called the Jones matrix of the link $\vec{E}(z) = \mathbf{U}(z)\vec{E}(0)$. The operation of a coherent transmission system requires that the receivers reconstruct in real time the full Jones matrix. The state of polarization is described a unit three-dimensional real vector called the Stokes vector, defined as $\vec{s}(z) = [\vec{E}(z)^\dagger \vec{\sigma} \vec{E}(z)]/\vec{E}(z)^\dagger \vec{E}(z)$, where we denoted by a dagger the hermitian conjugate of a vector. The tip of the Stokes vector lies on a unit sphere called the Poincaré sphere. The relation that links the output Stokes vector to the input Stokes vector is a three-dimensional rotation, $\vec{s}(z) = \mathbf{R}(z)\vec{s}(0)$ [7]. In the absence of perturbations, the rotation matrix $\mathbf{R}(z)$ is time independent. The use of a reference frame rotating with the static birefringence is equivalent of using a perfect compensator for the static birefringence at center frequency ω, and implies that in the absence of perturbations the output polarization at this frequency is equal to the input polarization, namely that $\vec{s}(z) = \vec{s}(0) = \vec{s}_0$. If we define $\vec{s} = \Delta\vec{s} + \vec{s}_0$, we obtain to first order for $\Delta s \ll 1$, the equation $\mathrm{d}\Delta\vec{s}/\mathrm{d}z = \Delta\vec{\beta}(z,t) \times \vec{s}_0$, which shows that only the component $\Delta\vec{\beta}_\perp$ of $\Delta\vec{\beta}(z,t)$ orthogonal to $\vec{s}_0$ is effective, and that $\Delta\vec{s}$ belongs to the plane orthogonal to $\vec{s}_0$. Solving this equation we obtain $\Delta\vec{s} = \int_0^z \Delta\vec{\beta}_\perp(z',t)\mathrm{d}z'$. Using $\Delta\vec{\beta} = \varepsilon\vec{\beta}$, and assuming that the time-dependent strain ε varies slowly, and deterministically, with z, we obtain $\Delta\vec{s} = \int_0^z \vec{\beta}_\perp(z')\,\varepsilon(t)\,\mathrm{d}z'$ which shows that the deviation of the SOP depends linearly on the time-dependent strain and is the basis of the sensing capabilities of a transoceanic cable.

Figure 1 shows, in the right panel, a spectrogram reporting the sum of the power spectral densities of the two components Δs_1 and Δs_2 of the vector $\Delta\vec{s}$ at the output of the Google-owned Curie cable [1] during the earthquake of $M_w = 6.2$ that occurred on May 22, 2020, 8.46 (UTC), with epicenter off coast of central Mexico. The Poincaré sphere has been rotated such that the vector $\vec{s}_0$, chosen as the average of the output Stokes vectors over the entire time span of one day, is parallel to the third axis of the Stokes space. The sampling time was 1s. The perturbation of the output polarization caused by the earthquake is clearly visible by the vertical, broadband, excitation marked

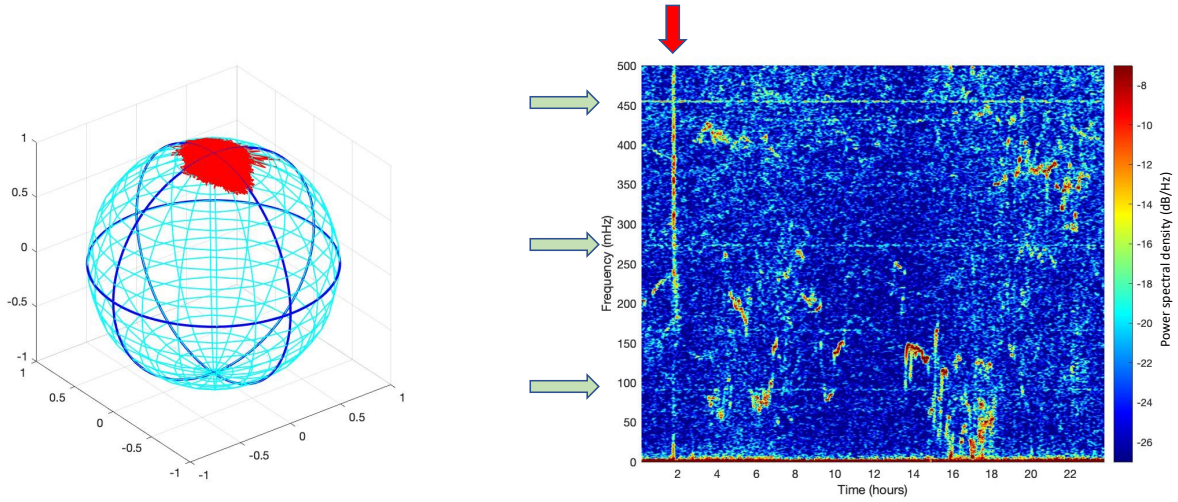

Fig. 1: Right panel: Spectrogram reporting the sum of the power spectral densities of the two components Δs_1 and Δs_2 of the vector $\Delta\vec{s}$ orthogonal to $\vec{s}_0$ of the output polarization of the Curie cable in the day of the earthquake of $M_w = 6.2$ that occurred on May 22, 2020, 8.46 (UTC), off coast of central Mexico. Abscissa is UTC–7 of May 22, 2020. Left panel: trajectory of the output polarization on the Poincaré sphere, rotated such that the average Stokes vector over the 24 hours time interval is centered on the North Pole. Red and green arrows: see text.

with a red arrow. The left panel shows the output of the Stokes vector over the Poincaré sphere during the same time interval. The fact that the tip of the vector, perturbed by an earthquake and over a one day time interval, never extends its trajectory outside a limited region around the North Pole, gives solid foundations to the use of linear spectral analysis for the study of the dynamics of Δs_1 and Δs_2. The green arrows point three spectral lines that show coherent excitation of the output SOP at frequencies $f_1 = 91$mHz, $f_3 = 273$mHz and $f_5 = 455$mHz. These values are typical of the series $f_{2n-1} = (2n-1)f_1$ originated by acoustic resonances in an oceanic layer of height H, with $f_1 = v_w/(4H)$ and $v_w \simeq 1500$m/s the speed of sound in water. The observed value of f_1 corresponds to a depth of 4.1km, which is the depth of the Curie cable in the vicinity of the earthquake's epicenter. The manifestation of these resonances shows the ability of a transoceanic cable to observe pressure variations that are coherent over the length scale of the cable, which is inaccessible to point-wise ocean-bottom pressure sensors. This highlights the potential of the analysis of SOP perturbations in transoceanic cables for the study of slow and coherent earth motions that may occur over tens or hundreds of kilometers scale.

References

1. Z. Zhan, M. Cantono, V. Kamalov, A. Mecozzi, R. Müller, S. Yin, and J. C. Castellanos, "Optical polarization–based seismic and water wave sensing on transoceanic cables," Science **371**, 931–936 (2021).
2. A. Mecozzi, M. Cantono, J. C. Castellanos, V. Kamalov, R. Muller, and Z. Zhan, "Polarization sensing using submarine optical cables," Optica **8**, 788–795 (2021).
3. M. R. Fernndez-Ruiz, M. A. Soto, E. F. Williams, S. Martin-Lopez, Z. Zhan, M. Gonzalez-Herraez, and H. F. Martins, "Distributed acoustic sensing for seismic activity monitoring," APL Photonics **5**, 030901 (2020).
4. A. Sladen, D. Rivet, J. P. Ampuero, L. De Barros, Y. Hello, G. Calbris, and P. Lamare, "Distributed sensing of earthquakes and ocean-solid earth interactions on seafloor telecom cables," Nat. Commun. **10**, 5777 (2019).
5. N. J. Lindsey, T. C. Dawe, and J. B. Ajo-Franklin, "Illuminating seafloor faults and ocean dynamics with dark fiber distributed acoustic sensing," Science **366**, 1103–1107 (2019).
6. H. Matsumoto, E. Araki, T. Kimura, G. Fujie, K. Shiraishi, T. Tonegawa, K. Obana, R. Arai, Y. Kaiho, Y. Nakamura, T. Yokobiki, S. Kodaira, N. Takahashi, R. Ellwood, V. Yartsev, and M. Karrenbach, "Detection of hydroacoustic signals on a fiber-optic submarine cable," Sci. Reports **11**, 2797 (2021).
7. J. P. Gordon and H. Kogelnik, "PMD fundamentals: Polarization mode dispersion in optical fibers," Proc. Natl. Acad. Sci. **97**, 4541–4550 (2000).
8. W. Urbanczyk, T. Martynkien, and W. J. Bock, "Dispersion effects in elliptical-core highly birefringent fibers," Appl. Opt. **40**, 1911–1920 (2001).
9. B. Budiansky, D. C. Drucker, G. S. Kino, and J. R. Rice, "Pressure sensitivity of a clad optical fiber," Appl. Opt. **18**, 4085–4088 (1979).
10. L. Schenato, A. Galtarossa, A. Pasuto, and L. Palmieri, "Distributed optical fiber pressure sensors," Opt. Fiber Technol. **58**, 102239 (2020).